Heat Capacity

- What does it take to cool down specimens?
- Stability of temperature against heat loads $\Delta T = \frac{1}{C}\Delta Q$
- Helps in calibrating thermometers
- Relationship between heat capacity and thermal conductivity
- Identify the nature of the system under study $C \propto T^n$
- Indicator for phase transitions in physical systems

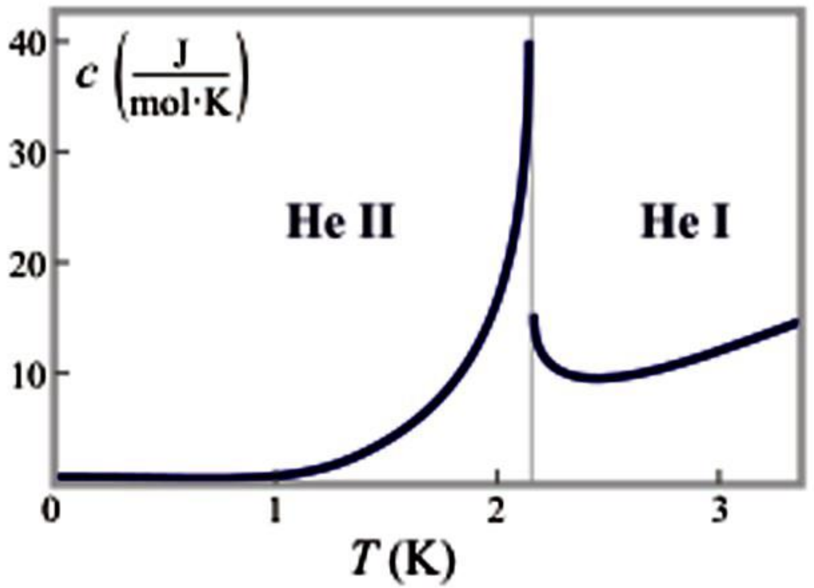

Sources:

P.V.E. McClintock, D.J. Meredith, and J.K. Wigmore, Low-Temperature Physics: an introduction for scientists and engineers (1992)

F. Pobell, Matter and Methods at Low Temperatures (2007)

Basic relations

Heat needed (dQ) to change temperature (dT)

– at constant volume: $C_V = (dQ/dT)_V$
– at constant pressure: $C_p = (dQ/dT)_p$

The difference between C_V and C_p is related to thermal expansion:

$C_p - C_V = 9\alpha^2\eta T,$ $$\alpha = \frac{1}{3}\left(\frac{\partial V}{\partial T}\right)_P = \frac{\gamma C_V}{3V\eta} \qquad \frac{\Delta\omega}{\omega} = \gamma\frac{\Delta V}{V}$$

(linear expansion coefficient α and bulk modulus η)
The difference becomes insignificant at low temperatures!

Heat capacity is related to entropy:

$$dQ = TdS\,;\;\; C = T\frac{dS}{dT}\,;\;\; S(T) = \int_0^T \frac{C}{T}\,dT$$

The integral remains finite only if $C \to 0$ when $T \to 0$

Sources of heat capacity

- Mobile entities
  - phonons (lattice vibrations)
  - conduction electrons in metals
  - gas or fluid particles (or quasiparticles)
  - ...
- Immobile entities
  - magnetic moments
  - electric dipoles or quadrupoles
  - tunneling states in amorphous lattice
  - ...

Heat capacity and thermal conductivity

Thermal conductivity κ_i (due to carrier type i) is proportional to heat capacity of the carriers (kinetic theory):

$$\dot{Q} = -\kappa A \nabla T$$

$$\kappa_i = \tfrac{1}{3} dU_i/dT_i \, v_i \ell_i = \tfrac{1}{3} C_i v_i \ell_i = \tfrac{1}{3} C_i v_i^2 \tau_i$$

$$\dot{Q} = \sum_{q} n'(\mathbf{q}) \hbar\omega(\mathbf{q}) v_x(\mathbf{q})$$

where v_i is the speed of the carriers (phonons, electrons, etc.), ℓ_i is their mean free path and $\tau_i = \ell_i / v_i$ is the mean collision time.

When heat capacity is due to mobile entities and the cooling time τ_0 is limited by the conductivity of the sample, τ_0 actually does not depend on heat capacity!

$$\tau_0 = R_i C_i \propto C_i / \kappa_i \propto \boxed{1/(v_i \ell_i)}$$

Determining factors are the speed and scattering properties of the carriers.

General method

Total energy $U = \int E \, dN/dE \, g(E) \, dE$
=> heat capacity $C = dU/dT$

To find the heat capacity of a given system
- identify the mechanism storing thermal energy
- deduce the dispersion relation
  * available states are often counted in reciprocal space *
- choose the proper distribution function $g(E)$
  (Boltzmann/Bose-Einstein/Fermi-Dirac)
- take care of proper normalization $N = \int dN/dE \, g(E) dE$
- determine the degeneracy factor
- evaluate average energy (energy/particle)
  * density of states dN/dE is needed *
- differentiate with respect of temperature (dg/dT)

Examples

Lattice vibrations (kinetic and potential energy of atomic nuclei)
- classical description is meaningful at high temperatures only
- Einstein's quantum hypothesis improves on that
- Debye's phonon model is more accurate at low T
- turnover occurs at "Debye temperature" $T_D \sim 100$ K

Conduction electrons in metals
- degenerate Fermi gas
- excitations only close to Fermi energy are important
- Fermi temperature $T_F = E_F / k_B \sim 10\,000$ K

Phonons and electrons can be treated separately
(Born-Oppenheimer approximation): $C = C_{ph} + C_{el}$
$*$ Note that T_{ph} may be different from T_{el} $*$

Phonons (background)

Simple model:

$$F_k^{\mathrm{L,R}} = \pm k\,(l - a)$$

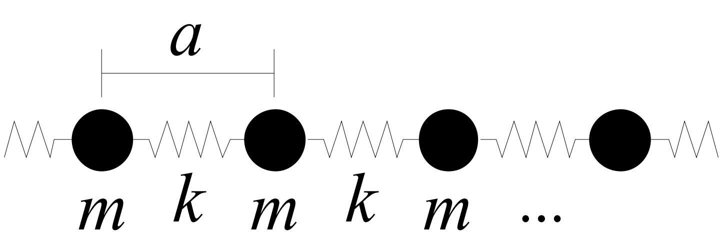

Equation of motion for particle n with displacement u_n:

$$m\, d^2u_n/dt^2 = k\,(u_{n+1} + u_{n-1} - 2u_n)$$

Try wave-like solution:

$$u_n = u_0\, \mathrm{e}^{\,\mathrm{i}\,(\omega t + q x_n)} \quad \Rightarrow e^{iqa}$$

Get dispersion relation:

$$\omega = \pm\, 2\,\sqrt{(k/m)}\,\sin\,(½qa)$$

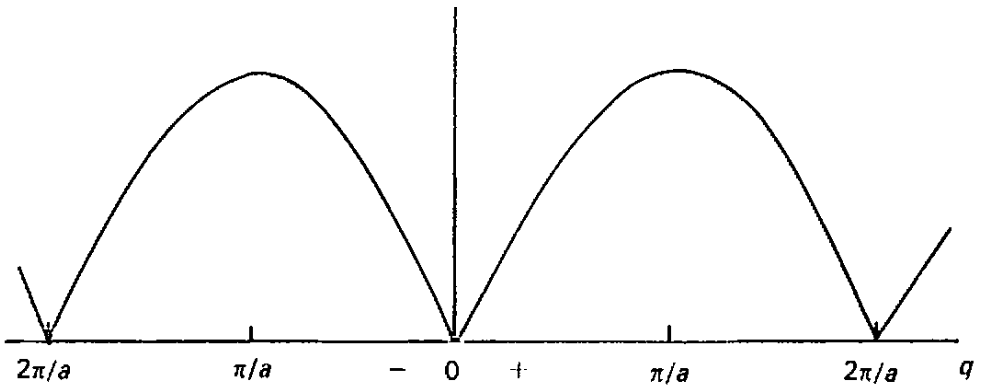

The dispersion curve of a ball-and-spring model of a one-dimensional monatomic lattice

Chain of atoms

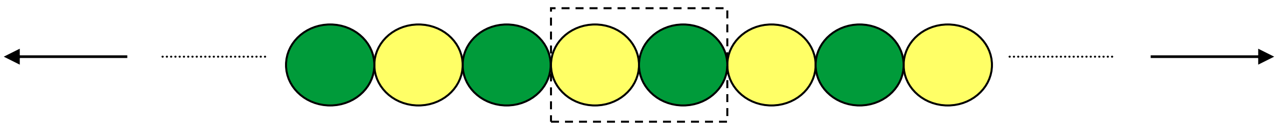

i

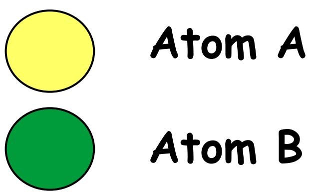

$$\hat{H} = \sum_i (E_{iA} c_{iA}{}^{\dagger} c_{iA} + E_{iB} c_{iB}{}^{\dagger} c_{iB} - t c_{iA}{}^{\dagger} c_{iB} - t c_{iA}{}^{\dagger} c_{i\text{-}1B} - t c_{iB}{}^{\dagger} c_{i+1A} + h.c.)$$

Hamiltonian Equation is :

$$\hat{H}|k\rangle = \begin{bmatrix} 0 & -t(1+e^{ika}) \\ -t(1+e^{-ika}) & 0 \end{bmatrix} \begin{bmatrix} u_A |k\rangle_A \\ u_B |k\rangle_B \end{bmatrix} = \varepsilon(k)|k\rangle$$

where,

$$|k\rangle = u_A |k\rangle_A + u_B |k\rangle_B$$

Solving the Secular Eqn:

$$\begin{vmatrix} -\varepsilon(k) & -t(1+e^{ika}) \\ -t(1+e^{-ika}) & -\varepsilon(k) \end{vmatrix} = 0$$

We obtain

$$\boxed{\varepsilon(k) = \pm\sqrt{2t(1+\cos(ka))}}$$

Two atom basis leads to the basic features of the graphene bandstructure

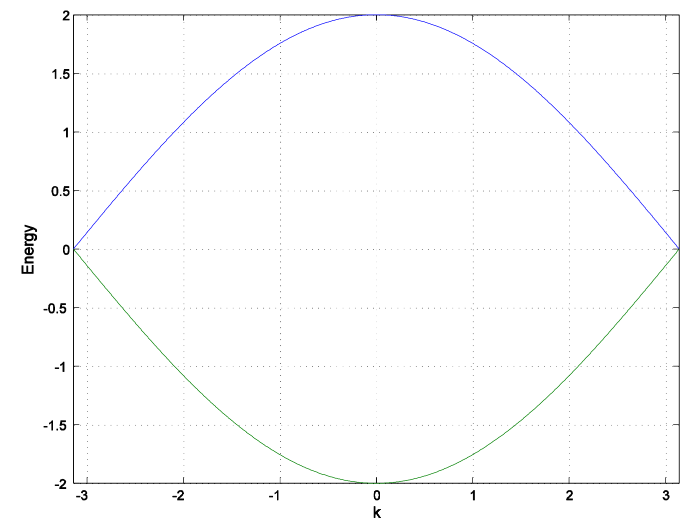

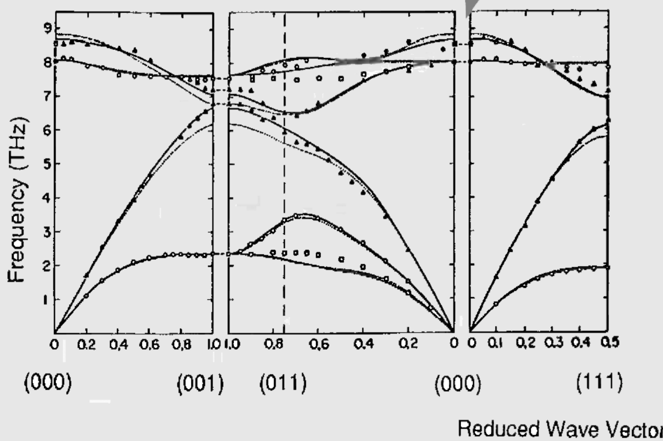

Figure 2.5 Phonon dispersion curves of GaAs determined by inelastic neutron scattering. The points (000) etc. refer to the reciprocal lattice directions of the phonons. (After Waugh and Dolling, 1963.) The curves refer to different lattice models.

Optical phonons do not contribute at low T

Thermal expansion can be neglected ($C_V = C_p$)

Harmonic approximation is excellent

Region of interest at low T

Group velocity:
$v_g = d\omega/dq = a\sqrt{(k/m)}$
(continuum approximation)

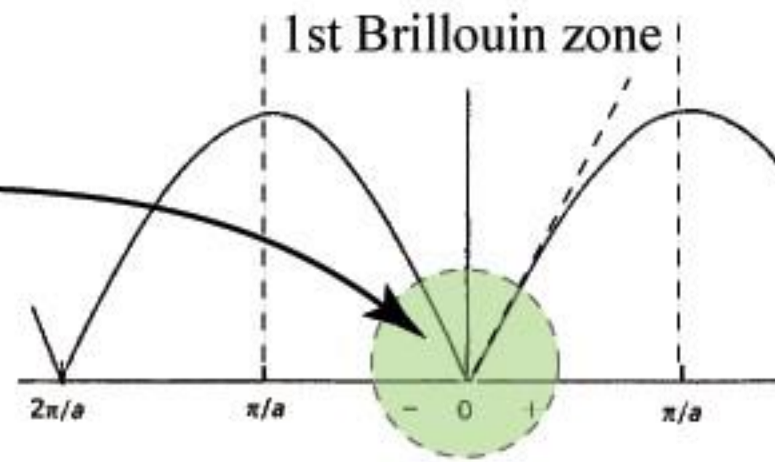

The dispersion curve of a ball-and-spring model of a one-dimensional monatomic lattice

Classical treatment

kinetic and potential energy:

$$E = \frac{1}{2} m \left(v_x^2 + \omega^2 x^2 \right)$$

Bolzmann distribution:

$$g(E) = e^{-E/k_B T}$$

Average energy:

$$\bar{E} = \frac{\int_0^\infty \int_0^\infty E \ \mathrm{e}^{-E/k_B T} dx\, dv_x}{\int_0^\infty \int_0^\infty \mathrm{e}^{-E/k_B T} dx\, dv_x}$$

3D (x, y, z) per mole (N_A):

$$U = 3 N_A \bar{E} \qquad \bar{E} = k_B T$$

Heat capacity:

$$C = \frac{dU}{dT} = 3 N_A k_B$$

$$= 24.94 \frac{\mathrm{J}}{\mathrm{mol\,K}}$$

3+3 degrees of freedom (kin+pot in 3D), ½ $k_B T$ each

=> Dulong-Petit law: $C = 3 N_A k_B$ (molar heat capacity)

Quantum viewpoint (Einstein)

energy as quanta in a set of harmonic oscillators:

$$E = (n + \frac{1}{2})\hbar\omega$$

Bose-Einstein distribution:

$$g(E) = \frac{1}{e^{\hbar\omega/k_B T} - 1}$$

Simple assumption: $\omega = \omega_E$ (Einstein 1907)

$$\bar{E} = (\frac{1}{\mathrm{e}^{\hbar\omega_E/k_B T} - 1} + \frac{1}{2})\hbar\omega_E$$

$$C = 3N_A k_B \frac{(\hbar\omega_E/k_B T)^2 \mathrm{e}^{\hbar\omega_E/k_B T}}{(\mathrm{e}^{\hbar\omega_E/k_B T} - 1)^2}$$

$U = \int E \, dN/dE \, g(E) \, dE$

$C = dU/dT$

Einstein's model

$$C = 3N_A k_B \frac{(\hbar\omega_E/k_B T)^2 e^{\hbar\omega_E/k_B T}}{(e^{\hbar\omega_E/k_B T}-1)^2}$$

Consistent with Dulong-Petit:

$$\underset{T\to\infty}{\longrightarrow} 3N_A k_B$$

Looks fine at intermediate temperatures

WHEN appropriate ω_E is chosen

Fails at $T \to 0$ (vanishes exponentially, i.e. too fast)

Heat capacity of diamond

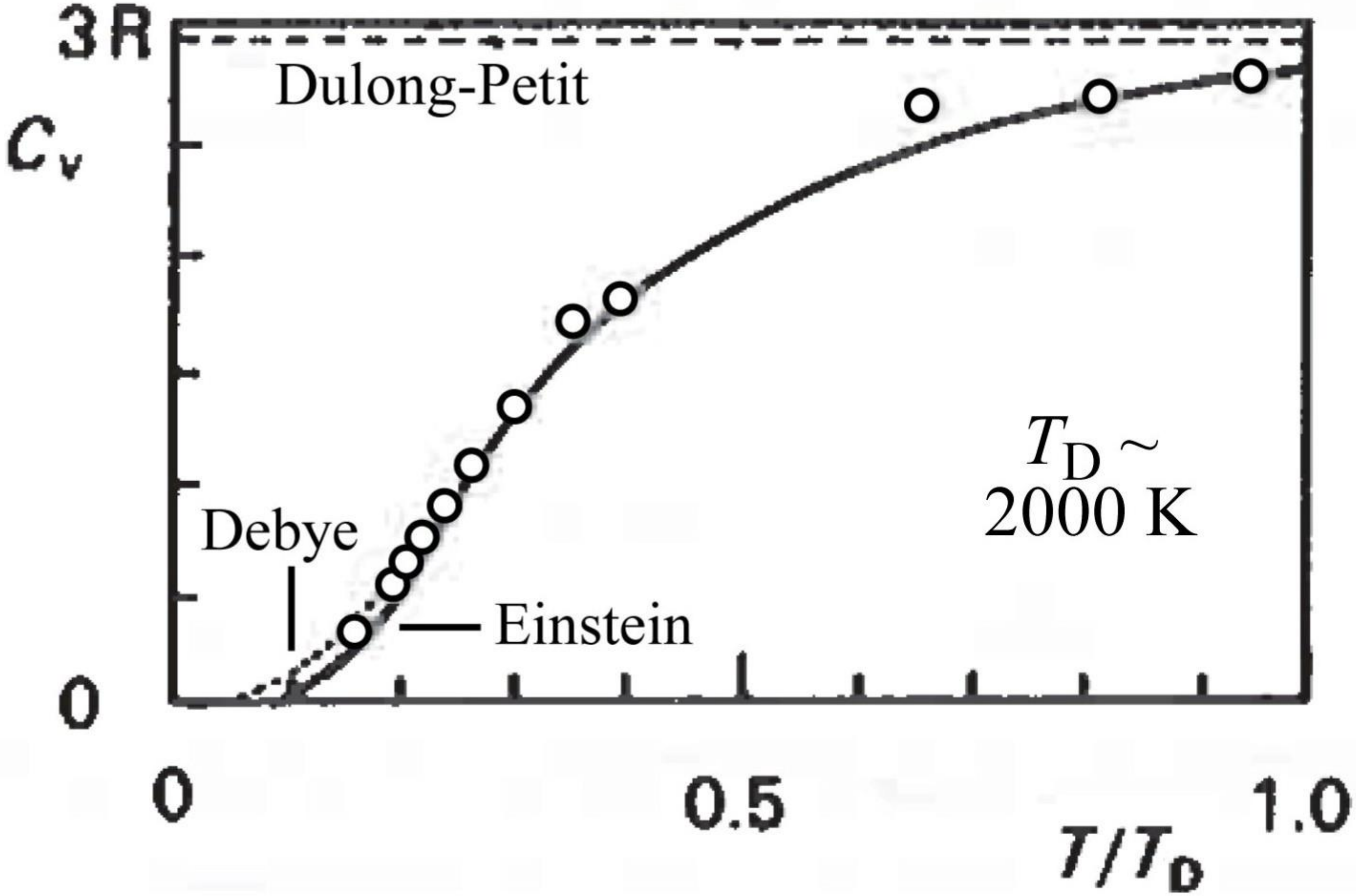

Figure 2.6 The original data on the low-temperature heat capacity of diamond used by Einstein (1907) to support his quantum theory of the heat capacity of solids. The data are compared with – – – – classical theory, ———— Einstein theory, and .... Debye theory.

Debye's theory

"phonons in a box" &
periodic boundary conditions

$$e^{i(q_1 x_1 + q_2 x_2 + q_3 x_3)} = e^{i[q_1(x_1+L)+q_2(x_2+L)+q_3(x_3+L)]}$$

$$e^{i(q_1 L + q_2 L + q_3 L)} = 1$$

$$q_i L = \pm 2\pi n \ , \quad q_i = 0, \ \pm\frac{2\pi}{L}, \ \pm\frac{4\pi}{L}, \ \ldots$$

... constant density of states
in q-space

$$1/(\frac{2\pi}{L})^3 = \frac{V}{8\pi^3}$$

Number of phonon modes (up to q):
(continuum approx. $\omega = v_g q$)
=> greatest needed $\omega = \omega_D$

$$N = \frac{4\pi}{3} q^3 \frac{V}{8\pi^3} = \frac{V\omega^3}{6\pi^2 v^3}$$

$$\omega_D^3 = \frac{6\pi^2 v^3 N}{V} \ ; \quad T_D = \frac{\hbar\omega_D}{k_B}$$

3 independent modes (2 transverse, 1 longitudinal)
N oscillators => $3N$ phonon modes
=> density of states

$$\frac{dN}{d\omega} = \frac{3V\omega^2}{2\pi^2 v^3}$$

Debye's result

phonon energy

$$U = \int_0^{\omega_D} \frac{dN}{d\omega} g(\omega) \hbar\omega \, d\omega$$

$$= \frac{3V\hbar}{2\pi v^3} \int_0^{\omega_D} \frac{\omega^3}{e^{\hbar\omega/k_B T} - 1} d\omega$$

& heat capacity

$$C = 9 N_A k_B \left(\frac{T}{T_D}\right)^3 \int_0^{T/T_D} \frac{x^4 e^x}{(e^x - 1)^2} dx$$

with

$$x = \frac{\hbar\omega}{k_B T}$$

Having

$$\int_0^{\infty} \frac{x^4 e^x}{(e^x - 1)^2} dx = \frac{4\pi^4}{15} \quad \underset{T\to 0}{=>} \quad C = \frac{12}{5}\pi^4 N_A k_B \left(\frac{T}{T_D}\right)^3$$

Real examples

$$\boxed{C \propto T^3}$$

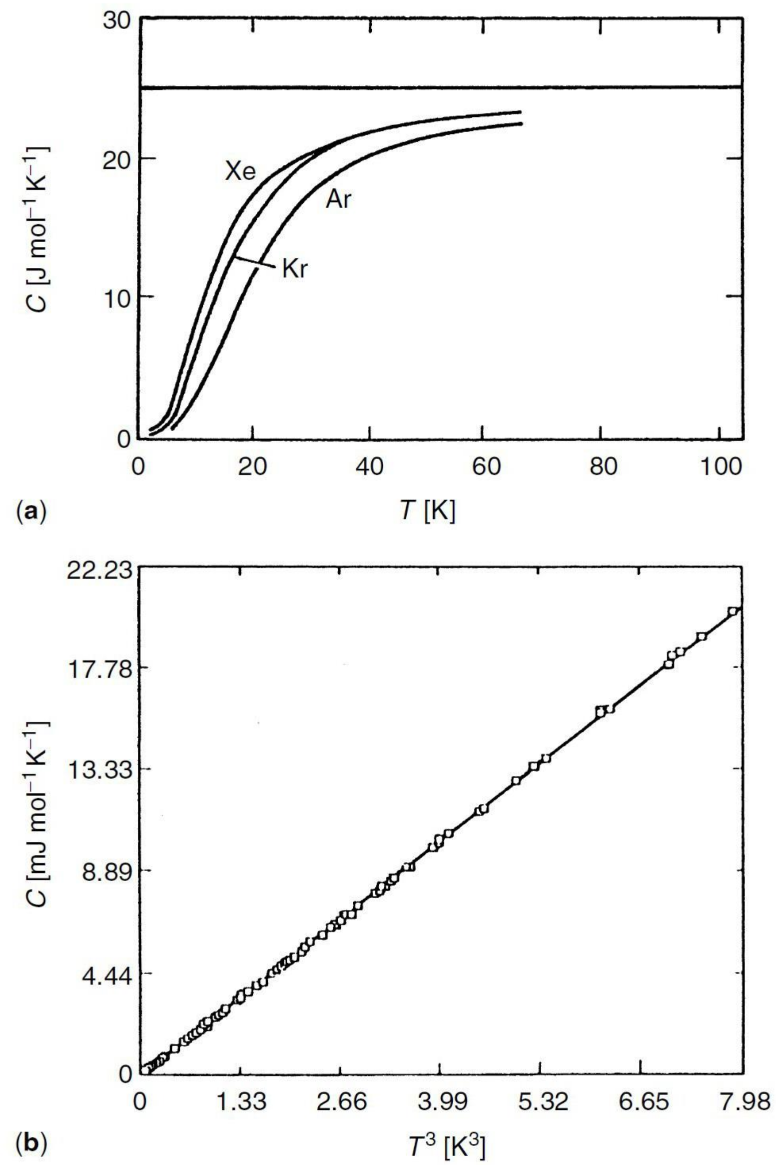

Fig. 3.2. (**a**) Specific heat of solid Ar, Kr and Xe. The horizontal line is the classical Dulong–Petit value [3.11]. (**b**) Specific heat solid of Ar as a function of T^3 at $T < 2\,\mathrm{K}$ [3.1, 3.12]

Conduction electrons

Free electron model, dispersion relation:

$$E_k = \frac{\hbar^2}{2m_e}|\bar{k}|^2$$

"electron waves in a box"

$$k_{x,y,z} = 0, \pm\frac{2\pi}{L}, \pm\frac{4\pi}{L}, \ldots \qquad (\Delta k)^d = \left(\frac{2\pi}{L}\right)^d$$

Fermi wavevector, - energy, - temperature (remember spin degeneracy)

$$k_F = \sqrt[3]{3\pi^2 N/V}\ , \quad E_F = \frac{\hbar^2}{2m_e}\left(\frac{3\pi^2 N}{V}\right)^{2/3}\ , \quad T_F = \frac{E_F}{k_B}$$

Density of states:

$$\frac{dN}{dE} = \frac{3}{2}N\sqrt{\frac{E}{E_F^3}} = \frac{m}{\pi^2\hbar^3}\sqrt{2mE}$$

Fermi-Dirac distribution ($\mu \sim E_F$):

$$g(E) = \frac{1}{e^{(E-\mu)/k_B T}+1}$$

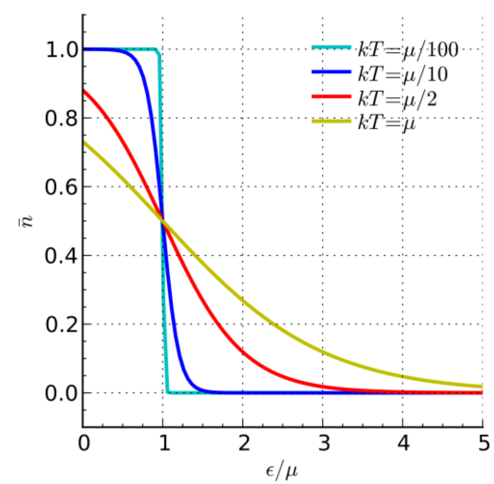

=> Sommerfeld result

collect the ingredients:

$$\int_{-\infty}^{\infty} \frac{H(\varepsilon)}{e^{\beta(\varepsilon-\mu)}+1}\,\mathrm{d}\varepsilon = \int_{-\infty}^{\mu} H(\varepsilon)\,\mathrm{d}\varepsilon + \frac{\pi^2}{6}\left(\frac{1}{\beta}\right)^2 H'(\mu) + O\left(\frac{1}{\beta\mu}\right)^4$$

$$C = \frac{dU}{dT} = \int_0^{\infty} E\,\frac{dN}{dE}\frac{dg}{dT}\,dE \approx \frac{\pi^2}{3}\frac{dN}{dE}\bigg\|_{E=E_F} k_B^2 T = \gamma T$$

For free electrons:

$$C = \frac{\pi^2}{2} N_A k_B \frac{T}{T_F}$$

The real situation is more complex but it boils down to evaluating the density of states at the Fermi surface!

$$\boxed{C = \gamma T}$$

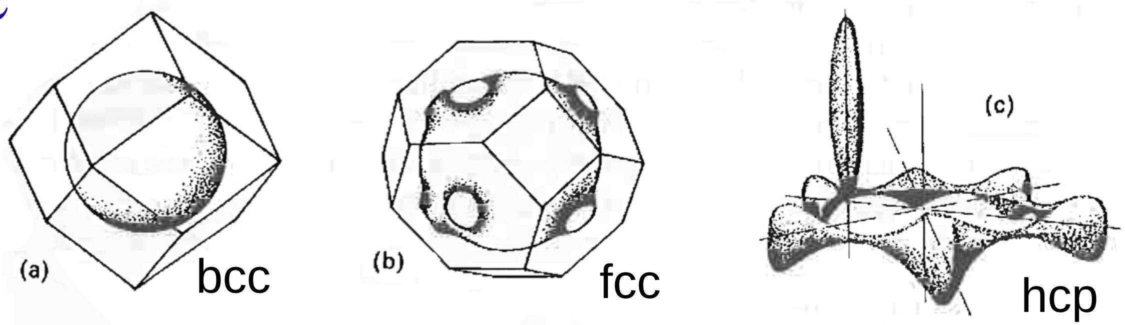

Figure 3.3 The Fermi surfaces of (*a*) potassium, body-centred cubic and monovalent: the Fermi surface is a free electron sphere to an accuracy of better than 1%; (*b*) copper, face-centred cubic and monovalent: the Fermi surface lies closer to the Brillouin zone boundary than for potassium and is distorted; (*c*) beryllium, hexagonal close-packed and divalent: electrons spill into the 2nd and 3rd Brillouin zones. The 'cigar' contains electrons, whilst the 'coronet' contains holes (Loucks and Cutler, 1964).

Examples

Contribution from both phonons & conduction electrons

$$C = \gamma T + \beta T^3 \quad \Rightarrow \quad \boxed{\frac{C}{T} = \gamma + \beta T^2}$$

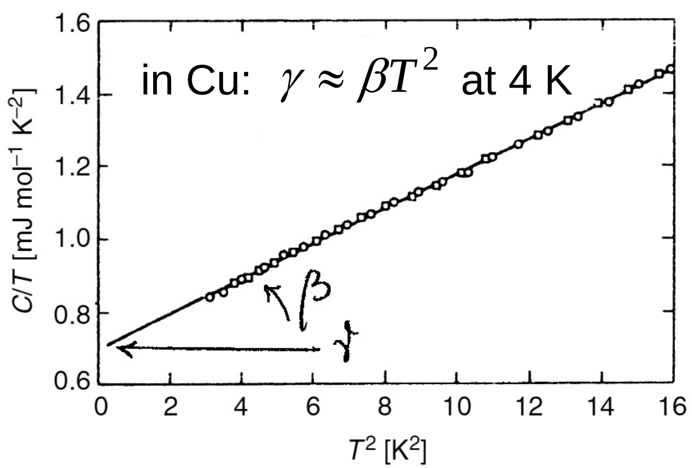

Fig. 3.4. Specific heat C of copper divided by the temperature T as a function of T^2 [3.4]

Properties of some metals. In some cases a mean average is given if two isotopes are present. For the two compounds included ($AuIn_2$ and $PrNi_5$) the data are for the element in italics.

isotope/ compound	ρ [g cm^{-3}]	V_m [cm^3 mol^{-1}]	θ_D [K]	γ [mJ mol^{-1} K^{-2}]	T_F [10^4 K]	$\rho_{273\,K}$ [μΩ cm]
^{27}Al	2.70	9.97	428	1.35	13.5	2.65
^{63,65}Cu	8.93	7.11	344	0.691	8.12	1.68
^{93}Nb	8.58	10.9	277	7.79	6.18	12.5
^{107,109}Ag	10.50	10.3	227	0.640	6.36	1.59
^{113,115}In	7.29	15.7	108	1.69	10.0	8.37
^{117,119}Sn	7.31	16.3	200	1.78	11.7	11.0
^{195}Pt	21.47	9.10	239	6.49	10.3	10.6
^{197}Au	19.28	10.2	162	0.689	6.41	2.24
^{203,205}Tl	11.87	17.2	78	1.47	9.46	18.0
AuIn_2	10.3	41.5	187	3.15	9.26	6.3
PrNi$_5$	8.0	51.0	230	40	–	80

Room temperature; phonons dominate
$T < 1$ K; conduction electrons dominate

$$C = \frac{\pi^2}{2} N_A k_B \frac{T}{T_F}$$

$$C = \frac{12}{5}\pi^4 N_A k_B \left(\frac{T}{T_D}\right)^3$$

Superconductors

Phonons – NO CHANGE

Electrons – JUMP at T_c

$\Delta C \approx 1.43\gamma T_c$

BCS supercond.

exp at $T < T_c$

$C \propto \mathrm{e}^{-b(T_c/T)}$

Carried by normal quasiparticles

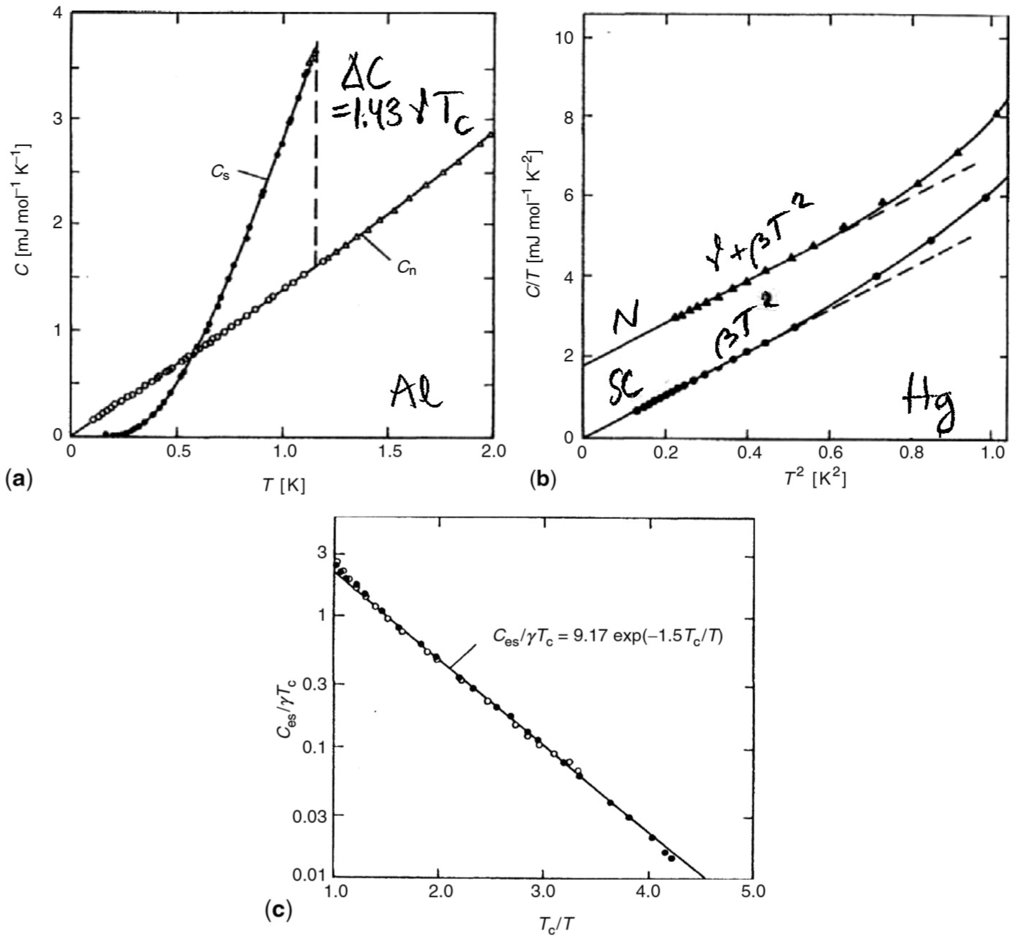

Fig. 3.5. (**a**) Specific heat of Al in the superconducting (C_s) and normal-conducting (C_n) states [3.20]. (**b**) Specific heat C of Hg divided by temperature T as a function of T^2 in the normal (▲) and superconducting (●) states. The straight lines correspond to (3.9,3.13) with $\theta_D = 72\,\mathrm{K}$ and $\gamma = 1.82\,\mathrm{mJ\,mol^{-1}\,K^{-2}}$ [3.21]. For the measurements in the normal conducting states, a magnetic field B > B_c had to be applied to suppress the superconducting state. (**c**) Electronic specific heat C_{es} of superconducting V (●) and Sn (○) divided by γT_c as a function of T_c/T. The full line represents (3.17) [3.22]

Amorphous solids

Tunneling between configurations of nearly equal energies is believed to be responsible for the heat capacity that remains at very low temperatures in amorphous solids, when the phonon contribution has practically vanished.

Empirically: $C_a = a\, T^n$

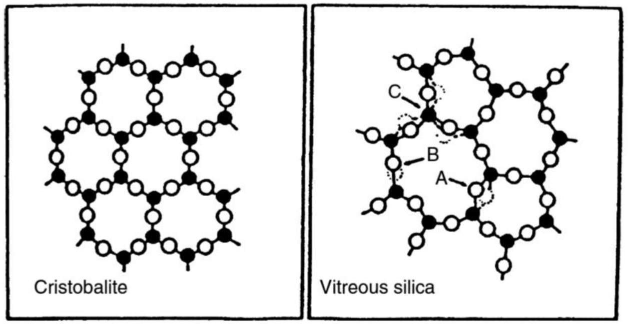

Fig. 3.6. Schematic two-dimensional representation of the structure of cristobalite, a crystalline modification of SiO_2, and of vitreous silica, the amorphous modification of SiO_2. Filled circles represent silicon atoms and open circles oxygen atoms. Three possible types of defects are indicated by arrows [3.5, 3.26]

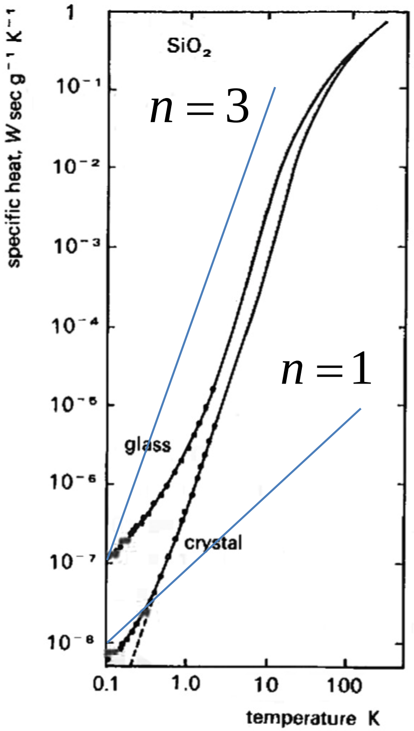

Figure 2.16 (*a*) The heat capacity of vitreous (amorphous) silica, compared with the data for crystalline quartz (Zeller and Pohl, 1971).

Liquid helium-4

Pronounced lambda-anomaly
at the superfluid transition
(resemblance with BEC)

Two-fluid model below T_λ
- superfluid part with $S = 0$
- normal component, finite C
- below $T \sim 0.5$ K just SF
  (phonons still exist => $C \propto T^3$)

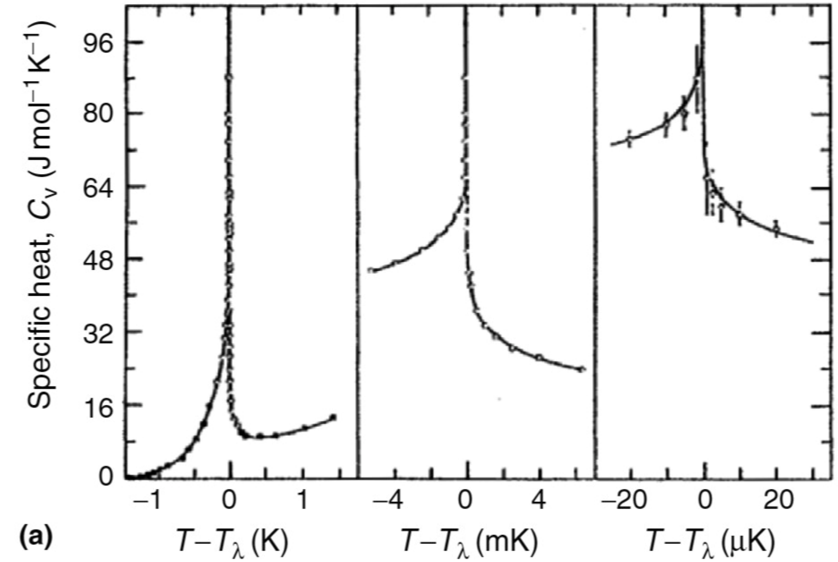

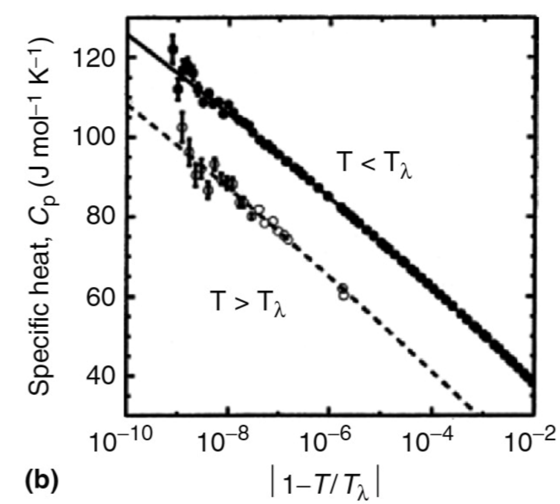

Fig. 2.10. Specific heat of liquid ^{4}He at temperatures close to its superfluid transition. (**a**) With increasing T-resolution on a linear temperature scale [2.27] and (**b**) on a logarithmic temperature scale. Reprinted with permission from [2.30]; copyright (2003) Am. Phys. Soc.. These latter data have been taken in flight on earth orbit to avoid the rounding of the phase transition by gravitationally caused pressure gradients in the liquid sample of finite height. For the applied high-resolution thermometry see Sect. 12.9

Liquid helium-3 & mixtures

^{3}He is a Fermi fluid
$T_F \sim 1$ K

Low-T behavior shows degenerate Fermi properties => $C \propto T$

Helium mixtures "interpolate" between the two but at very low temperatures (mK regime) the Fermi physics of the ^{3}He component always becomes dominant

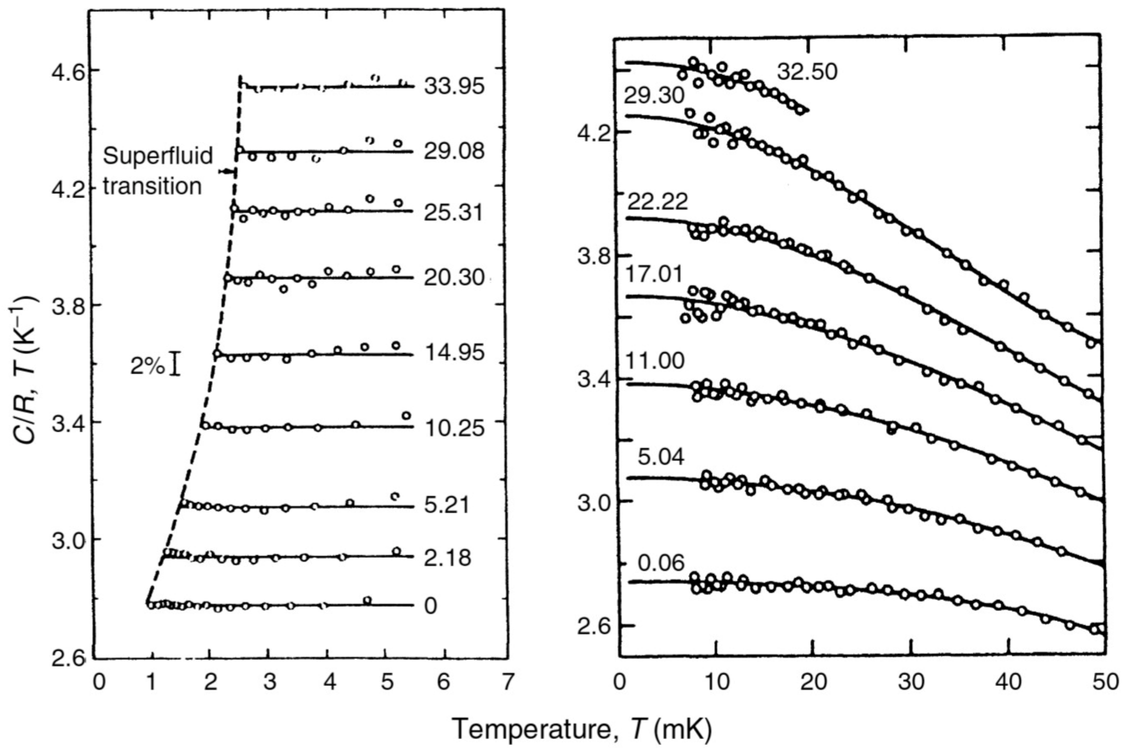

Fig. 2.15. Specific heat C divided by the gas constant R times temperature T of liquid ^{3}He at millikelvin temperatures at the given pressures (in bar). Note the different scales [2.26]

$$C = \frac{\pi^2}{2} N_A k_B \frac{T}{T_F}$$

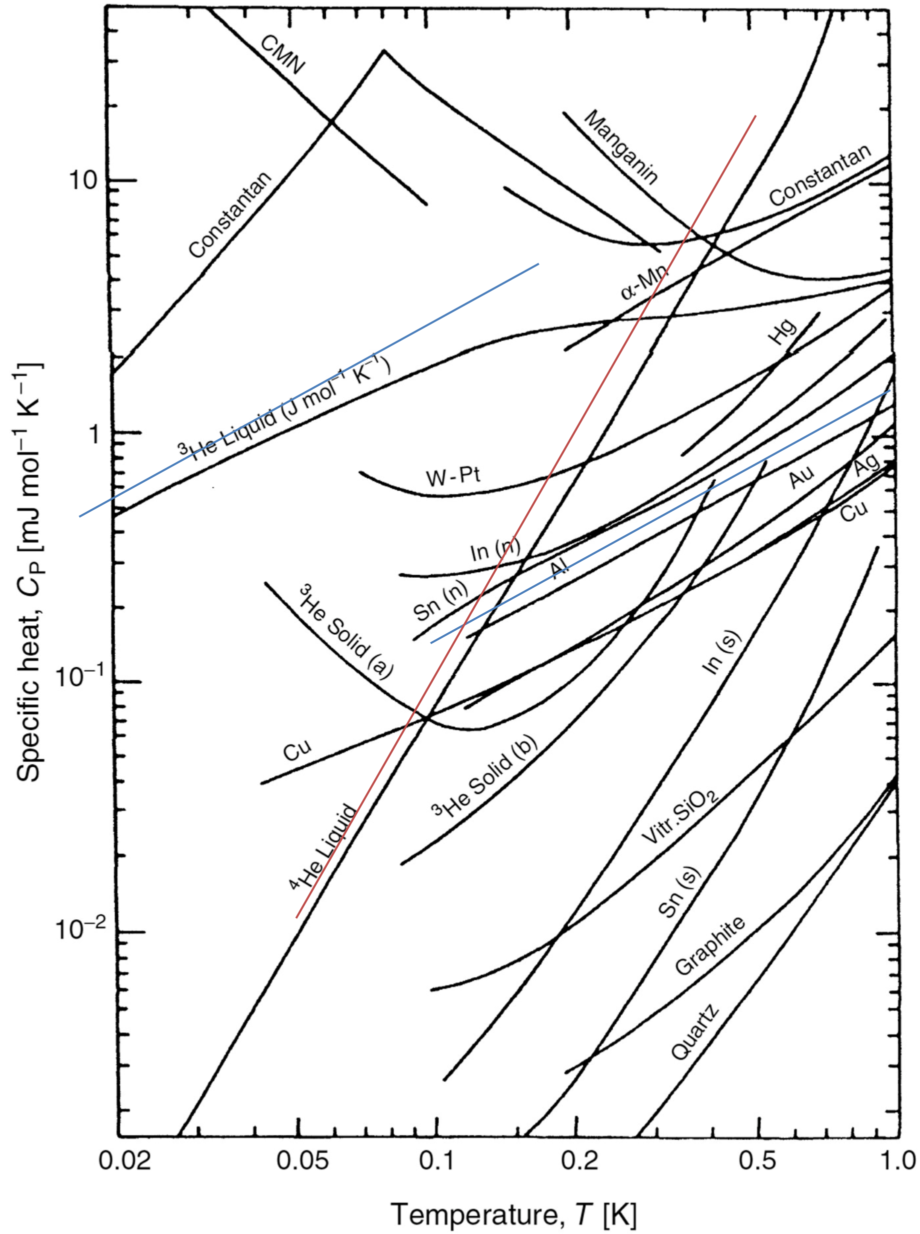

Fig. 3.12. Specific heats of several materials below 1 K [3.45]. (This publication provides references to the original literature)